The Fourth IEEE RAS/EMBS International Conference
on Biomedical Robotics and Biomechatronics
Roma, Italy. June 24-27, 2012

An Actuated Transfemoral Prosthesis with Optimized Polycentric Knee Joint

Serge Pfeifer, Robert Riener, and Heike Vallery

***Abstract*—Powered transfemoral prostheses can give above-knee amputees more flexibility than passive devices, for example allowing them to ascend and descend stairs more easily, or allowing a more natural and symmetrical gait pattern. To achieve the high torques required, most devices employ an electric motor with a ball-screw transmission, as is done in this work. The geometry of such a design determines how the peak torque is modulated as a function of joint angle. Therefore, it is important that this geometry is optimized to fulfill the requirements of the application. In this paper, we optimize this geometry to approximate a physiological peak torque versus joint angle versus joint velocity profile. Other powered knee prostheses commonly employ a single-axis joint. We investigate four different joint types: a single-axis joint, a biomimetic polycentric joint, a polycentric joint used in conventional passive prostheses, and an optimized polycentric joint. Our simulations suggest that employing an optimized polycentric joint can generate a uniform torque profile over the whole range of motion. An optimized geometry using a single-axis joint, however, can be used to obtain a peak torque versus angle profile that is similar to a physiological profile, and should, hence, be suitable for our application.**

I. Introduction

Active transfemoral prostheses like the PowerKnee (Össur, Reykjavik, Iceland) enable above-knee amputees to do activities that are not possible with passive devices (e.g. the C-Leg, Otto Bock, Duderstadt, Germany) without considerable compensatory torques in the hip joint. Such activities include standing up from a chair or ascending stairs with alternating legs. However, these activities require very high torques in the knee joint [1]. When using electric motors that are reasonably sized for this application, those high torques can only be obtained by a very high transmission, unless passive elements such as springs or dampers are added. This high transmission is usually achieved by using a ball-screw mechanism that transmits a linear force through a small lever to actuate a conventional hinge joint (e.g. Sup et al. [2]). In this inverted slider-crank mechanism, the transmission ratio is modulated with joint angle, and this modulation depends on the geometry of the design. As suitably sized electric motors work at their limits, it is important that this geometry is optimized. An appropriate geometry ensures that the requirements of the prosthesis can be fulfilled, and may potentially decrease the requirements on the motor.

The torque capabilities of a physiological knee joint depend on knee angle and on knee angular velocity [3], [4]. This is due to the changing moment arms about the joint [5], and the force-length and force-velocity relationship of muscle. The changing moment arms are caused in part by the polycentric nature of the knee joint, where the tibial condyles roll and slide back on the femoral condyles as the knee flexes, and the instantaneous center of rotation changes with knee angle [6]. This polycentric behavior can be approximated by a four-bar linkage, in which the cruciate ligaments form two of the bars [7].

For passive transfemoral prostheses, polycentric joints are widely used [8], often implemented as a four-bar linkage. The length of the four bars determines the trajectory of the instantaneous center of rotation. This trajectory is also called the centrode. It vastly differs from a physiological centrode (Fig. 1). The shape of the centrode influences how the motion of the prosthesis can be controlled by the user. For example, when the prosthetic knee is fully extended, the instantaneous center of rotation lies behind and above the actual knee joint, to increase the stability in stance phase [9]. Other advantages over single-axis joints are improved flexion cosmesis [10], and improved foot clearance [11].

In active prostheses, knee motion is controlled by the actuation unit, which is driven by some sort of user intention detection (e.g. Martinez-Villalpando and Herr [12]). This makes the need for a specifically shaped centrode obsolete. Rovetta et al. [13] have shaped the centrode to mimic the physiological knee joint, but an analysis of the advantages was missing. Furthermore, an arbitrary centrode could potentially be shaped to optimize the torque versus angle profile of the actuated joint.

When using a linear actuation concept such as an electric motor with a ball-screw transmission to drive the knee joint, the torque profile changes nonlinearly with the flexion angle of the joint (e.g. Semini et al. [14]). This profile is defined by the geometry of the design. Other groups developing active transfemoral prostheses have optimized their designs for different criteria. Sup et al. [15] minimized the actuator dimensions and the maximum force occurring during gait. Lambrecht and Kazerooni [16] did not specify in detail how the geometry was optimized. Martinez-Villalpando and Herr [12] used a different, antagonistic design with a focus on energy minimization during gait, without specifying details on the geometry. To our knowledge, no detailed analysis has been

This work was supported by the ETH Research Grant ETHIIRA, the Gottfried und Julia Bangerter-Rhyner Stiftung and the Swiss National Science Foundation through the National Centre of Competence in Research Robotics.

S. Pfeifer, R. Riener and H. Vallery are with the Sensory-Motor Systems Lab, ETH Zurich and Medical Faculty, University of Zurich, Switzerland (email: pfeifers@ethz.ch; hvallery@ethz.ch; riener@ethz.ch). H. Vallery is also with Khalifa University of Science, Technology & Research (KUSTAR), Abu Dhabi, UAE.

978-1-4577-1200-5/12/$26.00 ©2012 IEEE

reported where the torque profile was optimized explicitly to reflect the capabilities of a physiological knee.

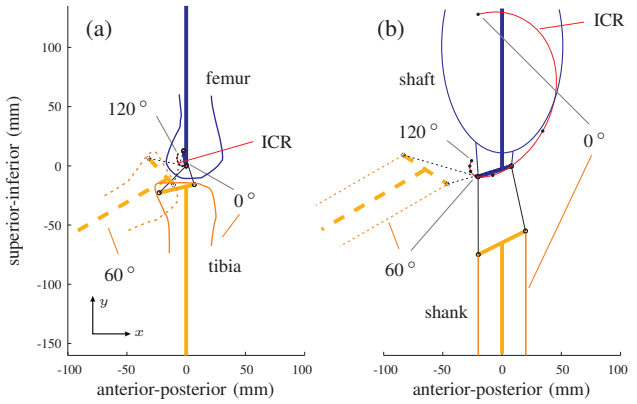

Fig. 1. Four-bar linkage knee joints. A biomimetic model (a) and a conventional polycentric knee joint (b). The trajectory of the instantaneous center of rotation (ICR) is depicted from 0 ° to 120 ° flexion, with black dots in intervals of 20 °.

In this paper, we develop an actuator concept that aims to approximate the peak torque versus angle versus angular velocity profile of a physiological knee joint. To achieve that goal, we optimize the geometry of a joint with linear actuation and investigate the effects of employing a single-axis joint and different polycentric joints.

II. Materials and Methods

Our goal was to approximate the capabilities of a physiological knee joint by a prosthetic joint that is driven by an electric motor through a ball-screw transmission, where the effective lever arm r_{eff} is modulated with joint angle (Fig. 2). This modulation depends on the geometry of the design. First, we selected appropriate components that should be able to achieve the requirements of a knee joint. Then, we optimized the geometry to achieve a peak torque versus angle versus angular velocity relationship close to the physiological knee. We used a single-axis joint, two predefined four-bar linkages, and also optimized the parameters of a four-bar linkage to better approximate the target torque profile.

A. Knee Joint Requirements

The requirements of a prosthetic knee joint are often deducted from normative gait data from the literature, for example during stair ascent and descent. These activities place high requirements on the knee joint and are also common for above-knee amputees. Data from unimpaired subjects are frequently used as a reference (e.g. Riener et al. [1]). Assuming the powered knee prosthesis would be used in combination with a passive ankle joint, knee data from below-knee amputees fitted with a passive ankle prosthesis could be used as a reference [17], [18]. During the same activity, the discrepancy in knee torque and power between unimpaired subjects and below-knee amputees is very high (Table I). Hence, it is difficult to deduct the requirements for a powered knee prosthesis from these data, especially when it could be used in combination with a passive or powered ankle.

To obtain more general requirements that are independent of a specific activity or prosthetic foot, we looked at the full possibilities of a physiological knee joint instead. Rather than in a table, these requirements are more comprehensively reflected in the the peak torque τ_{K} versus angle θ_{K} versus angular velocity $\dot{\theta}_{\text{K}}$ relationship of a physiological knee [3] (Fig. 3). Our goal was to approximate this profile by a powered knee prosthesis. If these requirements could be fulfilled, an above-knee amputee would theoretically be given the possibilities of a below-knee amputee.

The maximum mass of the device was based on a physiological shank and foot [19] (Table I). Furthermore, the device should be similar in size as a biological shank.

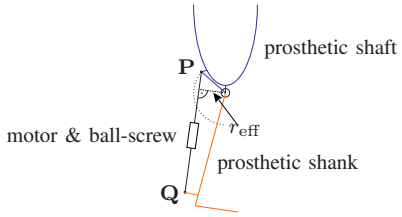

Fig. 2. Inverted slider-crank mechanism of a knee joint with linear actuation. The distance between the line of action of the linear actuator and the instantaneous center of rotation is denoted by r_{eff} (the effective lever arm). The attachment point at the shaft is denoted by $\mathbf{P}$, the attachment at the prosthetic shank by $\mathbf{Q}$.

TABLE I
Knee requirements based on stair ascent and descent of a nominal 70 kg subject (unimpaired and below-knee (BK) amputee). Root mean square (RMS) and peak values are reported for torque, power and velocity, depending on availability of data.

Quantity	Unimpaired	BK Amputee
Torque (Nm)	45 (RMS), 95 (peak) [1]	35 (peak) [17]
Power (W)	115 (RMS), -300 (peak) [1]	-120 (peak) [18]
Velocity (°/s)	200 (RMS), 500 (peak) [1]	–
Range of motion (°)	120	
Mass (kg)	4.3	

B. Motor and Transmission Requirements

Our calculations were based on the Maxon Powermax EC30 4-pole motor, due to its high power density, and a weight that is still acceptable for use in prostheses (200 W, 300 g). Its nominal power (200 W) is lower than for example the peak power during stair descent of unimpaired people (Table I). However, these peaks only occur during short periods of time, during which the motor can be overloaded and, hence, should be suitable for the application. The nominal speed of

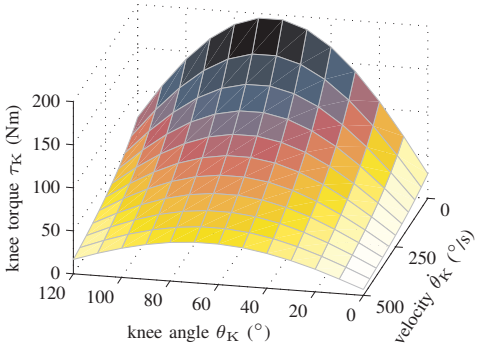

Fig. 3. Target torque versus angle versus angular velocity profile based on a physiological model of knee extension [3], assuming a male between 18 and 25 years, height 1.75 m, mass 70 kg.

the motor is 15800 rpm ($\omega_{\mathrm{M,n}} = 1655\,\mathrm{rad/s}$), a rotational speed that is too high for most ball-screws of acceptable size and weight. Hence, an additional transmission is needed. We assumed a belt drive with transmission ratio i, which is chosen such that 80 % of the critical speed of the ball-screw $\omega_{\mathrm{BS,crit}}$ was reached at the nominal speed of the motor:

$$i = \frac{\omega_{\mathrm{M,n}}}{0.8\omega_{\mathrm{BS,crit}}}, \tag{1}$$

At any time, the knee joint torque was given by

$$\tau_{\mathrm{K}} = \frac{\tau_{\mathrm{M}} 2\pi i}{l} r(\theta_{\mathrm{K}}) \tag{2}$$

and the angular velocity by

$$\dot{\theta}_{\mathrm{K}} = \frac{\omega_{\mathrm{M}} l}{2\pi i} \frac{1}{r(\theta_{\mathrm{K}})}, \tag{3}$$

where l denotes the lead of the ball-screw, τ_{M} the torque of the motor, ω_{M} the rotational speed of the motor, and $r(\theta_{\mathrm{K}})$ is the effective moment arm about the center of rotation at the knee angle θ_{K}. Losses in the transmission or ball-screw were neglected. To select a suitable ball-screw and transmission ratio i, we first ensured that the maximum joint angular velocity could be achieved. The maximum necessary joint angular velocity was assumed to be $500\,^\circ/\mathrm{s}$ ($\dot{\theta}_{\mathrm{K,max}} = 8.7\,\mathrm{rad/s}$) (Table I). The maximum linear velocity depends on the lead l of the ball-screw:

$$v_{\mathrm{BS,max}} = \frac{\omega_{\mathrm{M,n}} l}{i}. \tag{4}$$

This yields an upper bound for the allowed effective moment arm acting about the joint center:

$$r_{\max} = v_{\mathrm{BS,max}} / \dot{\theta}_{\mathrm{K,max}} \tag{5}$$

Very small moment arms lead to high forces acting on the ball-screw. To avoid damaging the ball-screw independently from control precautions, we placed a lower bound on the effective lever arm based on the maximum permissible force $F_{\mathrm{BS,perm}}$ acting on the ball-screw:

$$r_{\min} = \tau_{\mathrm{K,peak}} / F_{\mathrm{BS,perm}}, \tag{6}$$

where the peak torque $\tau_{\mathrm{K,peak}}$ was assumed to be 150 Nm/rad, which corresponds approximately to the peak torque of a 100 kg unimpaired person during stair descent [1]. The selection of the ball-screw was a trade-off between the desires to achieve a large range $r_{\max} - r_{\min}$ and a low weight. Based on this trade-off, we selected a 12 x 5 ball-screw (diameter 12 mm, lead 5 mm, Nook Industries, Cleveland, Ohio). This yielded a transmission $i = 3.1$, $v_{\mathrm{BS,max}} = 0.42\,\mathrm{m/s}$, $r_{\max} = 48.5\,\mathrm{mm}$, $r_{\min} = 12.5\,\mathrm{mm}$. For low velocities, we assumed the motor could be overloaded up to four times the nominal torque of $\tau_{\mathrm{M,n}} = 0.118\,\mathrm{Nm}$ for low velocities. This resulted in a maximum force produced by the ball-screw of $F_{\mathrm{BS,max}} = 1845\,\mathrm{N}$ (neglecting losses in the transmission). When the instantaneous power of the motor exceeded twice the rated power of $P_{\mathrm{M,n}} = 200\,\mathrm{W}$, the maximum motor torque was further reduced, depending on the required velocity. This resulted in an available torque for the motor of

$$\tau_{\mathrm{M,max}} = \min\left(4\tau_{\mathrm{M,n}}, 2P_{\mathrm{M,n}}/\omega_{\mathrm{M}}\right), \tag{7}$$

and the joint angular velocity could always be achieved (see Eq. 4, 5).

Based on these parameters, we optimized the geometry of the prosthesis to approximate the peak physiological torque versus angle versus angular velocity profile [3].

C. Optimal Geometry of a Linear Actuator

A ball-screw transmission driven by an electric motor provides a linear force independent of the current nut position. When it drives an inverted slider-crank mechanism with constant force, it produces a nonlinear torque profile at the actuated joint, as the effective lever arm r_{eff} changes with the joint angle (Fig. 2). This torque profile is modulated by the attachment points $\mathbf{P}$ and $\mathbf{Q}$ of the transmission. We optimized these points to yield a torque profile that is similar to a physiological torque profile. With the assumptions above, we minimized the squared difference between the target torque profile $\tau_{\mathrm{K,tg}}$ [3] (Fig. 3) and the torque profile τ_{K} that resulted from the different attachment points $\mathbf{P}$ and $\mathbf{Q}$:

$$J(\mathbf{P},\mathbf{Q}) = \sum_i \sum_j \left(\tau_{\mathrm{K}}\left(\theta_{\mathrm{K},i}, \dot{\theta}_{\mathrm{K},j}\right) - \tau_{\mathrm{K,tg}}\left(\theta_{\mathrm{K},i}, \dot{\theta}_{\mathrm{K},j}\right)\right)^2,$$
$$\forall\, i,j \quad \tau_{\mathrm{K}}\left(\theta_{\mathrm{K},i}, \dot{\theta}_{\mathrm{K},j}\right) < \tau_{\mathrm{K,tg}}\left(\theta_{\mathrm{K},i}, \dot{\theta}_{\mathrm{K},j}\right). \tag{8}$$

We used a grid optimization that contained all combinations of coordinates of $\mathbf{P} = (P_x, P_y)$ and $\mathbf{Q} = (Q_x, Q_y)$ within the bounds $P_x, Q_x \in [-5\,\mathrm{cm}, 5\,\mathrm{cm}]$, $P_y \in [-3\,\mathrm{cm}, 3\,\mathrm{cm}]$ and $Q_y \in [-30\,\mathrm{cm}, P_y - 5\,\mathrm{cm}]$ in steps of 1 cm. We used this grid optimization because more sophisticated optimization methods would have become computationally too challenging, in particular for the case of a four-bar linkage, as described in the following section, where 8 additional parameters need to be found. The coordinates are given in the global coordinate frame (x is anterior-posterior and y is superior-inferior) when the knee joint is completely extended and the leg standing vertically, with the origin of the coordinate frame where the prosthetic shank and shaft intersect. In the case of a single-axis joint, this origin lies exactly on the joint axis.

D. Employing a Four-Bar Linkage Joint

In a four-bar linkage joint, the instantaneous center of rotation changes as the joint angle θ_{K} changes. When driven by a linear actuation, this has an effect on the effective moment arm r_{eff} acting about the joint. By choosing appropriate linkage parameters, $r_{\mathrm{eff}}(\theta_{\mathrm{K}})$ can be shaped more flexibly compared to a single-axis joint. To achieve this, we used the same formalism as Hobson and Torfason [20] to opimize a four-bar linkage, which has 8 free parameters (A_x, A_y, B_x, B_y, a_1, a_2, a_3, α_0, see Fig. 4) and only allows linkages that fulfill the Grashof criterion [21]. By employing such a joint instead of the single-axis joint, the cost function (Eq. 8) now depended on 12 parameters. We calculated all possible combinations of the parameters on a discrete grid of 1 cm resolution within the bounds: $A_x \in [-2\,\mathrm{cm}, 2\,\mathrm{cm}]$, $B_x \in [A_x + 1\,\mathrm{cm}, 2\,\mathrm{cm}]$, $A_y, B_y \in [-5\,\mathrm{cm}, 2\,\mathrm{cm}]$, $a_1, a_2, a_3 \in [1\,\mathrm{cm}, 4\,\mathrm{cm}]$, and the the same bounds as above were used for P_x, P_y, Q_x, Q_y. These bounds keep the size of the prosthetic knee joint within reasonable limits. The angle α_0 was adjusted in steps of 20 ° over the whole range of 360 °.

Apart from this optimization, we also investigated the effect of a physiological centrode (Fig. 1a), and the use of a conventional four-bar linkage joint employed in passive prostheses (Fig. 1b). Because the range of the centrode was much higher in the conventional four-bar linkage, it was necessary to increase the upper bound for the allowed effective

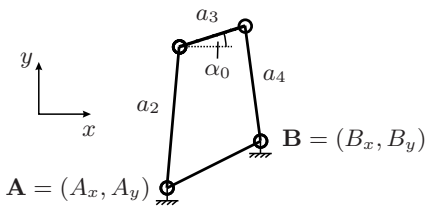

Fig. 4. Four-bar linkage parameters.

moment arm $r_{\max}$ (Eq. 5). This was done by multiplying $r_{\max}$ by factor three, which can be seen as increasing the lead of the ball-screw by factor three. Due to its inversely proportional dependence on the lead, the maximum achievable linear force was consequently divided by factor three. For the two predefined four-bar linkages (biomimetic and conventional passive prosthesis), the 8 parameters of the linkage were given, which reduced the number of optimized parameters to four, the same amount as with the single-axis joint.

To quantify the performance of the different geometries, we calculated the volume spanned between the surface of the physiological torque profile and the surface resulting from the optimized geometry at angles and velocities where the physiological profile exceeded the capabilities of the prosthetic joint. This value differed from our cost function (Eq. 8), where the squared difference is used. We then normalized the obtained value by the total volume spanned by the surface of the physiological torque profile.

III. Results

The optimization yielded very different geometries (attachment points **P** and **Q**) for the different joints (Fig. 5). For the optimized four-bar joint, the ball-screw was placed behind the knee joint (Fig. 5a). The instantaneous center of rotation traveled from the front at 0 ° flexion to the back of the thigh at 120 ° flexion on an almost horizontal path. With a single-axis joint, the optimal geometry using our criterion placed the ball-screw diagonally from the back of the shaft to the front of the shank (Fig. 5b). Using a biomimetic four-bar, the resulting placement of the ball-screw was entirely in front of the leg (Fig. 5c). The conventional four-bar linkage yielded the largest distance between the two attachment points (Fig. 5d).

The torque profiles resulting from the optimized geometries matched the physiological capability for many combinations of knee angle and knee velocity, and even exceeded it for some. However, under the assumptions we made for the motor and transmission, none of profiles came close to the maximum physiological knee torque at low velocities in the middle of the knee range of motion, or the peak isometric torque (194.7 Nm). The geometry with the optimized four-bar linkage yielded a flatter torque profile (Fig. 6a) than the other linkages, and the highest peak torque (89.4 Nm when $\theta_{\mathrm{K}} = 100\,^{\circ}, \dot{\theta}_{\mathrm{K}} = \{0\,^{\circ}/\mathrm{s}, \ldots, 250\,^{\circ}/\mathrm{s}\}$). Much of the total volume spanned by the physiological target profile was reached, only 16.5 % could not be achieved by the actuator. The geometry with the single-axis joint yielded a torque profile similar in shape as the physiological profile (Fig. 6b), with a peak torque of 82.5 Nm when $\theta_{\mathrm{K}} = 70\,^{\circ}, \dot{\theta}_{\mathrm{K}} = \{0\,^{\circ}/\mathrm{s}, \ldots, 250\,^{\circ}/\mathrm{s}\}$. The volume not achieved by the actuator was higher than for the optimized four-bar linkage (24.2 % of the physiological volume). The

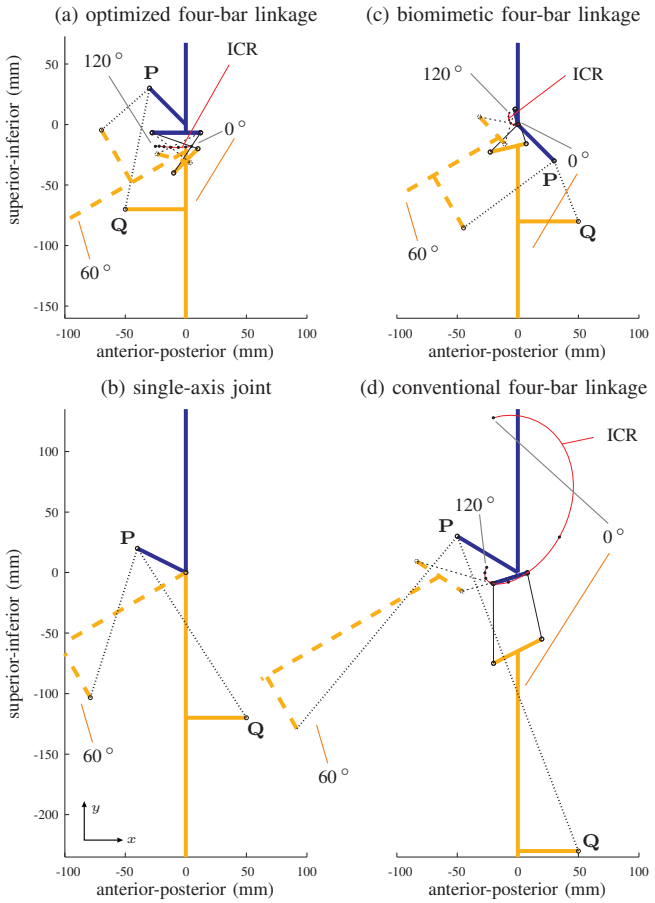

Fig. 5. Optimized geometry for knee joints actuated by a ball-screw (dotted lines connecting **P** and **Q**) for an optimized four-bar linkage (a), a single-axis joint (b), a biomimetic four-bar linkage (c), and a conventional four-bar linkage prosthetic knee joint [9] (d). The prosthetic shaft and shank, and rigidly attached elements are sketched in vertical position at 0 ° flexion angle (thick solid lines). The shank and rigidly attached elements are also sketched at 60 ° flexion (thick dashed lines). The trajectory of the instantaneous center of rotation (ICR) is depicted from 0 ° to 120 ° flexion, with black dots in intervals of 20 °.

TABLE II
Optimized attachment points and linkage parameters (Fig. 5). All parameters are given in mm except α_0 (in °).

configuration	P_x, P_y	Q_x, Q_y	A_x, A_y	B_x, B_y	a_2	a_3	a_4	α_0
optimized four-bar	-30,30	-50,-70	-10,-40	10,-20	40	40	40	180°
single-axis joint	-40,20	50,-120	-	-	-	-	-	-
biomimetic four-bar	30,-30	50,-80	-22.8,-22.7	6.9,-15.9	32.2	12.8	29.9	100°
conventional four-bar	-50,30	50,-230	-20.1,-75.0	19.8,-55.0	65.9	29.3	56.0	17.6

torque profile resulting from the geometry with the biomimetic four-bar linkage slightly exceeded the torque profile using the single-axis joint (Fig. 6c). Its peak was 85.3 Nm when $\theta_{\mathrm{K}} = 60\,^{\circ}, \dot{\theta}_{\mathrm{K}} = \{0\,^{\circ}/\mathrm{s}, \ldots, 250\,^{\circ}/\mathrm{s}\}$. Of the total volume spanned by the target profile, 21.1 % could not be achieved using this geometry. The torque profile using the conventional four-bar linkage differed the most from the physiological profile (Fig. 6d). Its peak occurred in a very different configuration ($\theta_{\mathrm{K}} = 10\,^{\circ}, \dot{\theta}_{\mathrm{K}} = \{0\,^{\circ}/\mathrm{s}, \ldots, 350\,^{\circ}/\mathrm{s}\}$), and was much lower (61.7 Nm). As much as 62.2 % of the volume spanned by the target profile was not reached using this joint and geometry.

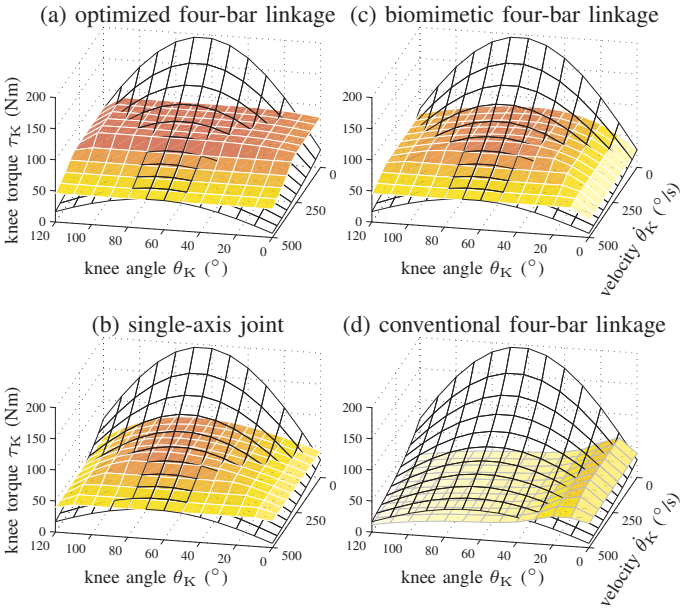

Fig. 6. Torque versus angle versus angular velocity profiles for optimized actuator geometries (Fig. 5) depicted as solid surface. The target torque profile (Fig. 3) is depicted as transparent mesh for reference.

IV. Discussion

In this paper, we investigated how the torque profile of an actuated knee prosthesis can be optimized. For a joint with linear actuation, for example an electric motor with a ball-screw transmission, this profile depends on joint angle and joint velocity. It was our hypothesis that a prosthetic knee should approximate the torque profile of a physiological knee. Based on requirements obtained from normative gait data, we selected appropriate components and then optimized the geometry. The attachment of the linear actuator was optimized for different types of joints. We examined the effects on the torque profile of a single-axis joint, a biomimetic four-bar linkage, a conventional prosthetic four-bar linkage joint, and a four-bar linkage with optimized parameters.

The optimization yielded qualitatively different geometries for the different joint types (Fig. 5). While we reported the optimal configurations, it could make sense to select a sub-optimal configuration for practical reasons. For example, the ball-screw needs to provide sufficient travel, which could be problematic, for example, for the optimal geometry using a single axis joint (Fig. 5a); above the attachment point on the shaft, there is no space for the ball-screw to retract, and as both attachment points approach each other for high flexion angles, the ball-screw could potentially stick out of the shank, which is undesirable with respect to cosmesis. To tackle this problem, one could manually select a more practical geometry out of the ones with similar cost, or one could add additional constraints in the optimization.

Our selection of motor, transmission, and constraints guaranteed that the high knee joint velocities during stair ambulation of unimpaired subjects could be reached for all geometries. But none of the geometries was able to reach the high peak torques a physiological knee can achieve in isometric contractions, it was approximately 60 % lower. Compared to peak torques occurring during stair ambulation of unimpaired subjects, the peak torques produced by three out of our four geometries (Fig. 6 a, b, c) were only 6-13 % lower (Table I), and these peaks occurred at similar knee angles (around 60 ° flexion). The torques occurring during stair ambulation of below-knee amputees could easily be achieved, which should be comparable to the situation where the powered knee prosthesis is used in combination with a passive ankle joint.

Our results were based on the assumption that the peak torque of the motor is its nominal torque times four, which is a rather conservative assumption [22]. The assumed restriction on motor peak torque was the limiting factor for knee peak torque up to velocities of 250 °/s, for higher velocities the constraint we applied on maximum power was the limiting factor (Eq. 7). However, the stall torque of the motor is factor 7 higher than our assumption (almost factor 30 higher than its rated torque). Hence, even the high knee torques during stair ambulation of unimpaired subjects (Table I) could most likely be achieved, and, very briefly, even the peak torque values of a physiological knee at stall could be achievable for three out of the four geometries (Fig. 6 a, b, c). The exact torque that can be achieved depends on many factors though, namely the duration of the overload, winding and ambient temperatures and the mounting of the motor. When using the powered knee in combination with a passive ankle prosthesis, a situation comparable to a below-knee amputee fitted with a passive ankle prosthesis, the torques in the knee joint during stair ambulation should be easily reached (Table I).

Our final design will employ the concept of a series-elastic actuator [23], where an elastic element is placed between the actuator and the load, in order to protect the actuator and transmission from shocks and to allow accurate force control. This increases the velocity requirements of the actuator. For a first conservative approximation, the higher velocity required can be calculated as the required torque gradient divided by the stiffness of the joint. Assuming values from the literature for peak required torque gradient (approximately 1000 Nm/s during physiological stair ascent [1]) and for required stiffness (up to 600 Nm/rad [24]), the required velocity is approximately 100 °/s higher than without the elastic element. This corresponds to only 20 % of the maximal velocity we guaranteed by our constraints. Hence, our geometries could likely be used unaltered if the maximum torque gradient does not occur at times where the peak velocity is needed, or they could be minimally modified by moving the linear actuator closer to the knee center to reduce the effective lever arm about the joint. This would also decrease the peak joint torque, a decrease proportional to the reduction of the lever arm.

For a commercial prosthesis, energy efficiency is a major concern, which we did not address in this work. To improve energy efficiency, and potentially lower the requirements on the motor, it would be beneficial to add passive elements in parallel to the actuator. During level-ground walking and stair descent, knee power is mainly dissipative [1]. Hence, a damper could provide most of the torque during these tasks. Furthermore, springs could be used to store and release energy, which would also increase the peak output torque of the prosthesis. However, these measures would increase the

complexity of the device. Here we derived design parameters for a simple and lightweight prototype suitable for various activities in a lab environment. The value of additional passive elements will be evaluated in future work.

Four-bar linkage mechanisms have already been used in active knee prostheses. However, the designs aimed to mimic a physiological centrode [13], [25], and the consequences it has for the actuated prosthesis were not analyzed. Here we presented a detailed analysis of the effects on the torque profile of such a biomimetic joint with linear actuation, and we compared it to other joint types.

A single-axis joint driven by a linear actuator yielded a torque profile similar in shape as a physiological profile, and given our conservative assumptions, would most likely be suitable in a transfemoral prosthesis. The smaller peak torque that was achieved compared to the optimized four-bar linkage was probably due to the coarse grid used in the optimization, which did not allow the single-axis geometry to exhaust the effective lever arm up to the upper bound that was used. Compared to a biomimetic four-bar linkage, the differences were negligible. Using our assumptions and constraints, a conventional four-bar linkage prosthetic joint with linear actuation did not seem feasible. For an optimized four-bar linkage, the resulting torque profile was almost flat over the whole range of motion (Fig. 6a). This indicates an almost constant effective lever arm, which was expected from this geometry, because the instantaneous center of rotation moves backwards as the knee flexes, and the linear actuator also moves backwards (Fig. 5a). While a flat torque profile is not physiological, amputee gait patterns differ from physiological patterns, and uniform torque capabilities could be beneficial. How knee torques of transfemoral amputees with an active prosthesis differ from torques in physiological gait patterns most likely depends on the prosthetic foot used, and the control strategy of the prosthesis. Without extensive experiments investigating these effects, it is difficult to predict whether the additional complexity of a four-bar linkage is justified, and an optimized geometry with a single-axis joint seems suitable to assess these effects.

V. Conclusion

Optimizing the geometry of a linearly actuated single-axis joint yielded a peak torque versus angle profile similar to the profile of a physiological knee. Using an optimized four-bar linkage instead of a single-axis joint resulted in an almost uniform torque profile over the range of motion of the knee. While exact requirements on the torque profile of a prosthetic knee are difficult to predict and depend on the control strategy used and the prosthetic foot, it seems reasonable to approximate a physiological profile and to use an optimized geometry with a simple single-axis joint. In future work, the constraints of our optimization may be revisited to facilitate the design of the device, and a series-elastic element will be added to protect the transmission from shocks and to allow accurate force control.

References

[1] R. Riener, M. Rabuffetti, and C. Frigo, "Stair ascent and descent at different inclinations," *Gait & Posture*, vol. 15, no. 1, pp. 32–44, 2002.

[2] F. Sup, H. A. Varol, J. Mitchell, T. J. Withrow, and M. Goldfarb, "Preliminary evaluations of a self-contained anthropomorphic transfemoral prosthesis," *IEEE/ASME Trans. Mechatronics*, vol. 14, no. 6, pp. 667–676, 2009.

[3] D. E. Anderson, M. L. Madigan, and M. A. Nussbaum, "Maximum voluntary joint torque as a function of joint angle and angular velocity: Model development and application to the lower limb," *J. Biomech.*, vol. 40, no. 14, pp. 3105 – 3113, 2007.

[4] K. Khalaf, M. Parnianpour, and T. Karakostas, "Three dimensional surface representation of knee and hip joint torque capability," *Biomed. Eng.: App. Bas. C.*, vol. 13, no. 2, pp. 53–65, 2001.

[5] J. Buford, W. L., J. Ivey, F. M., J. D. Malone, R. M. Patterson, G. L. Pearce, D. K. Nguyen, and A. A. Stewart, "Muscle balance at the knee-moment arms for the normal knee and the ACL-minus knee," *IEEE Trans. Rehabil. Eng.*, vol. 5, no. 4, pp. 367 –379, dec 1997.

[6] G. L. Smidt, "Biomechanical analysis of knee flexion and extension," *J. Biomech.*, vol. 6, no. 1, pp. 79 – 92, 1973.

[7] J. J. O'Connor, T. L. Shercliff, E. Biden, and J. W. Goodfellow, "The geometry of the knee in the sagittal plane," *Proc. Inst. Mech. Eng. H J. Eng. Med.*, vol. 203, no. 48, pp. 223–233, Sep. 1989.

[8] K. R. Kaufman, J. A. Levine, R. H. Brey, B. K. Iverson, S. K. McCrady, D. Padgett, and M. Joyner, "Gait and balance of transfemoral amputees using passive mechanical and microprocessor-controlled prosthetic knees," *Gait & Posture*, vol. 26, no. 4, pp. 489 – 493, 2007.

[9] C. W. Radcliffe, "Biomechanics of knee stability control with four-bar prosthetic knees," in *ISPO Australia Annual Meeting*, 2003.

[10] J. W. Michael, "Modern prosthetic knee mechanisms," *Clinical Orthopaedics and Related Research*, vol. 361, pp. 39–47, 1999.

[11] S. A. Gard, D. S. Childress, and J. E. Uellendahl, "The influence of four-bar linkage knees on prosthetic swing-phase floor clearance," *JPO: Journal of Prosthetics and Orthotics*, vol. 8, no. 2, pp. 34–40, 1996.

[12] E. C. Martinez-Villalpando and H. Herr, "Agonist-antagonist active knee prosthesis: A preliminary study in level-ground walking," *J. Rehabil. Res. Dev.*, vol. 46, no. 3, pp. 361–374, 2009.

[13] A. Rovetta, X. Wen, and F. Cosmi, "Realization of a prosthesis of the lower limb: Development of kinematics," *Robot. Cim.-Int. Manuf.*, vol. 8, no. 3, pp. 137 – 142, 1991.

[14] C. Semini, N. G. Tsagarakis, E. Guglielmino, M. Focchi, F. Cannella, and D. G. Caldwell, "Design of HyQ a hydraulically and electrically actuated quadruped robot," *Proc. Inst. Mech. Eng. I J. Syst. Control Eng.*, vol. 225, no. 6, pp. 831–849, 2011.

[15] F. Sup, A. Bohara, and M. Goldfarb, "Design and control of a powered transfemoral prosthesis," *Int. J. Rob. Res.*, vol. 27, no. 2, pp. 263–273, 2008.

[16] B. G. A. Lambrecht and H. Kazerooni, "Design of a semi-active knee prosthesis," in *IEEE Int. Conf. on Robotics and Automation*, 2009, pp. 639–645.

[17] T. Schmalz, S. Blumentritt, and B. Marx, "Biomechanical analysis of stair ambulation in lower limb amputees," *Gait & Posture*, vol. 25, no. 2, pp. 267 – 278, 2007.

[18] M. Alimusaj, L. Fradet, F. Braatz, H. J. Gerner, and S. I. Wolf, "Kinematics and kinetics with an adaptive ankle foot system during stair ambulation of transtibial amputees," *Gait & Posture*, vol. 30, no. 3, pp. 356 – 363, 2009.

[19] D. A. Winter, *Biomechanics and Motor Control of Human Movement*, 2nd ed. New York: Wiley, 1990.

[20] D. A. Hobson and L. E. Torfason, "Optimization of four-bar knee mechanisms a computerized approach," *J. Biomech.*, vol. 7, no. 4, pp. 371 – 376, 1974.

[21] R. S. Hartenberg and J. Denavit:, *Kinematic Synthesis of Linkages*. McGraw-Hill, New York, 1964.

[22] Maxon Motor. http://www.maxonmotorusa.com/. June 1, 2011, [Jan. 18, 2012].

[23] G. A. Pratt and M. M. Williamson, "Series elastic actuators," in *IEEE/RSJ Int. Conf. on Intelligent Robots and Systems*, vol. 1, 1995, pp. 399–406.

[24] S. Pfeifer, M. Hardegger, H. Vallery, R. List, M. Foresti, R. Riener, and E. J. Perreault, "Model-based estimation of active knee stiffness," in *Conf. Proc. IEEE Int. Conf. Rehabil. Robot.*, 2011, pp. 1 –6.

[25] M. Karami, G. Maurice, and J. M. Andre, "A model of exo-prosthesis of the knee optimized with respect to the physiological motion of condyles," *ITBM-RBM*, vol. 25, no. 3, pp. 176 – 184, 2004.